

# Autonomous Solar Power Plant for Household Applications

Md. Hazrat Ali  
School of Engineering, Nazarbayev University,  
Astana, Kazakhstan  
Email: md.ali@nu.edu.kz

N. Mir-Nasiri  
School of Engineering, Nazarbayev University,  
Astana,  
Kazakhstan

**Abstract**—The aim of this project is to design and develop an efficient and autonomous small scale solar power plant for household application. The efficiency of the system is enhanced by the implementation of microcontroller based sun tracking system. The problem of panel overheating is designed to be eliminated by the usage of heat sink layer, acrylic glass, and natural air cooling. In addition, the objective of the research is to design the system so that it is able to operate in an autonomous mode. In other words, automatic switch between two charges is constructed. It is implied that the power plant is capable to be installed in rural areas as well as in urban environment, and with minimum human interference and technical maintenance. Therefore it is a significant issue to develop a system available to sustain the whole cycle of operations starting from sunlight harvesting, conversion into electrical energy, and finishing with power storage and distribution processes.

**Keywords**—Renewable; energy; tracking; household

## I. INTRODUCTION

The continuous increase of energy consumption and mineral resource depletion put the issue of sustainable power supply at first place. On the other hand, the use of conventional energy sources such as coal, oil and gas has become one of the main topics being actively discussed worldwide. The major concern is the environmental impact of these power sources such as decrease of ozone layer thickness, global warming, increase of concentration of carbon dioxide and other hazardous gases and chemicals in air and water, which in turn result in significant increase of chronic diseases [1]. Basically, the amount of solar energy received by surface of the Earth depends on movement of the Sun and the Earth ( Fig.1). For instance, in midday the solar radiation reaches its maximum, compared to energy received in dawn (sunrise) and dusk (twilight) periods. It is explained by the fact that at midday the location of the Sun is on zenith, i.e. far above the horizon, hence the length of the path passed by sun rays becomes shorter, consequently, less solar radiation is scattered and absorbed and more reaches the surface of the planet[2].

Moreover, as mentioned before, the geographic location is also a significant factor affecting the sunlight harvesting. For example, near the equator the solar energy received is obviously more compared to the poles: in Central Europe, Middle Asia and Canada the solar radiation is about 1000kWh/m<sup>2</sup>, in the Mediterranean it is almost 1700kWh/m<sup>2</sup>, and in desert areas of Africa, Middle East and Australia this values goes up to 2200kWh/m<sup>2</sup> [3]. Along with this, there is another geographic phenomenon affecting the amount of energy generated by solar panels. Clouds are the major objects defining how much energy is actually received by the planetary surface, as they significantly decrease the sunlight harvesting. The geographic objects such as mountains, seas, oceans, and large lakes are likely to trigger the formation of massive clouds. Other anthropogenic and natural phenomenon such as smog and ash also tend to deteriorate the exposure of the surface of the panel to sunlight. Therefore, these aspects should be taken into consideration during the selection of potential site for installation of solar power plant.

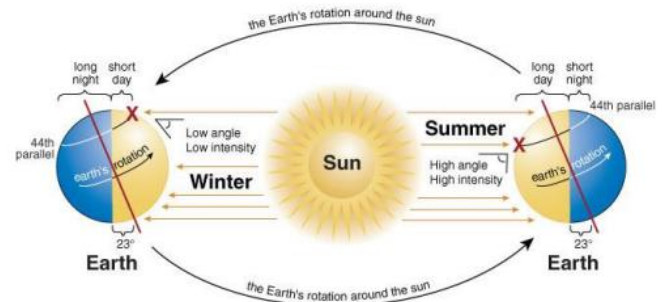


**Fig. 1.** Annual Sun orientation

The conversion of solar radiation into useful energy might be done through application of both active and passive systems. The active systems are solar collectors and photoelectric elements; whereas passive system is designing the building and usage of materials (natural room lightning, thermal isolation materials) so that it maximizes the usage of sunlight. The amount of solar radiation received

is directly related to Milankovitch cycles, which are eccentricity of Earth's orbit, obliquity (axial tilt) of the planet and precession (orientation of rotational axis). Consider Figure 1.3 demonstrating the annual sun path in the local area of Astana, Kazakhstan [4]. Due to fact that the region is located north of the equator, and noting an axial tilt of the Earth of about  $23.4^\circ$ , the coverage of sun radiation lies in the range of  $120-165^\circ$ . As expected, the maximum path of the Sun corresponds to summer (June 21st) and the shortest path corresponds to winter (December 21st). As it was noted, the most important property of a solar panel is the power output, which directly depends on the intensity of light the panel is exposed to, i.e. the brighter the light (higher luminosity) the more current is generated by photo elements [5]. Figure 1.5 shows the maximum efficiency of the solar battery is achieved if the sun tracking process is carried out in both horizontal and vertical axes. Nevertheless [6] states that the horizontal sun tracker itself also demonstrates quite good performance compared to a fixed panel. Therefore, considering the annual sun path in the local area, the horizontal axis sun tracking might be a good alternative.

## II. PROTOTYPE DEVELOPMENT

### A. Mechanical system design

However, this design was rejected due to the power output difference between top and bottom stack of solar panels are very large. The tested result is available in Chapter 6 of this report. Besides, temperature rise would also affect the efficiency and further lowers power output. Meaning to say, a cooling system would have to be implemented into such design. However, due to the limitation of structure design, it would be too difficult to incorporate such a cooling system. After some analysis and discussions between supervisor and team members, the result is a new design as shown in Fig. 2.

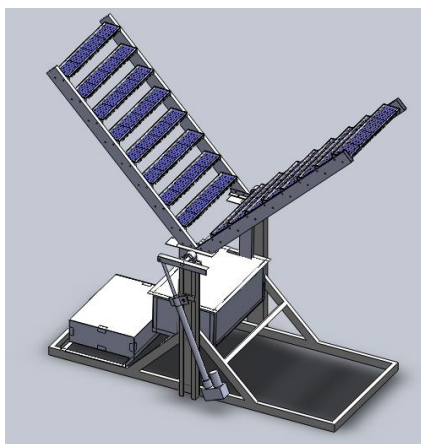


Fig. 2. Conceptual design of the target solar pane

### B. Electrical and electronics component design

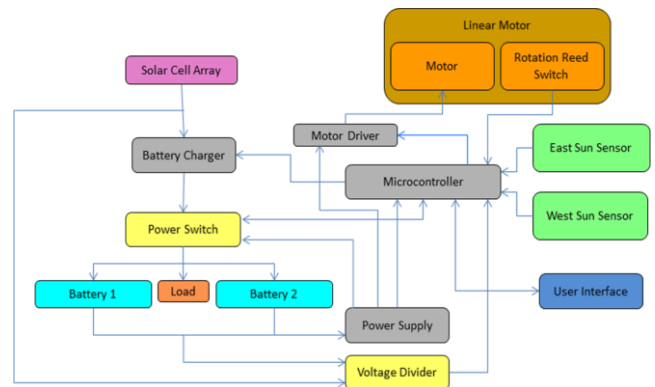


Fig. 3. Block diagram the electronics and electrical system

The mobile solar power station has a sun tracking feature to maximize solar power accumulation. A linear motor attached to the structure as described in previous mechanical section and a couple of sun tracking sensors are utilized as output and input respectively for the tracking. Accumulated power will be stored in two large capacity batteries configured as buffer while supplying out to application load at the same time. The batteries were monitored full time for optimum charging condition to prolong the lifetime. Power management and regulation circuitry is also a necessity to ensure stable power supply to other circuitry of the system. Figure 3 shows the proposed block diagram of the electronics and electrical system.

### C. Battery

The two batteries selected for use in this project are MSB branded with model number MS 12-18. These batteries are Valve Regulated Lead Acid (VRLA) batteries, designed for low maintenance usage. Each battery has a capacity of 18Ah at 12V voltage. The label on the batteries stated two charging modes with different charging voltage. The first is the Boost Charge which specifies charging voltage in between 14.5V to 15.5V. Second is the Equalize Charge with voltage from 12.8V to 13.8V. This project requires the batteries to be charged quickly to store more power when sunlight is available so Boost Charge mode is preferred. However, Boost Charge mode would only be safe when temperatures of batteries are below  $40^\circ\text{C}$  [7].

### D. Controller circuit

The controller circuit is based on a programmable microcontroller with a number of drivers and conditioning circuits. Compare to analog control circuits, digital control using a microcontroller allows for flexibility, short design and development time and precision control. Recent advancement and popularity of microcontrollers has resulted with a wide

variety of selections that are suitable for almost any kind of controller projects. The improvements in microcontroller manufacturing technology had also produced microcontrollers with very low power consumption. This is beneficial to the project as the controller will be required for non-stop operation and not taxing out much of the accumulated power. Full schematic of the circuit can be found in Appendix B.

A Microchip PIC16F887 8-bit microcontroller has been selected as the base of the controller circuit. This microcontroller has the most important “nanoWatt Technology” low power consumption feature for the controller of this project. The required components for this microcontroller to operate could also be minimized as it has a software selectable 8MHz precision internal oscillator built in. On the peripheral, it contains a 10-bit analog to digital converter with 14 channels of input, 10-bit pulse width modulation module, 35 inputs or outputs, and three timers. Special features of the microcontroller are low power watchdog timer for microcontroller program crash reset and power saving sleep mode with ultra-low power wakeup. Figure 3.4 shows the microcontroller with the corresponding pin connections.

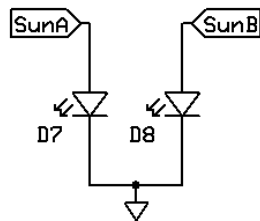


**Fig. 4.** LED sensors

The LEDs in **Fig. 4** are the sensing elements for sun tracking. LEDs with transparent optical case were selected as they allow more light to reach the semiconductor in it. Available transparent optical case LEDs in local market are red, green, blue, amber and white LEDs. Among the five colors, red and amber are most sensitive followed by green, blue and white. Under a 25W LED white light array, red and amber LEDs reached saturated forward voltage and change on the light angle in extreme only produces very small voltage difference. Blue LED falls in the suitable output voltage range but low linearity throughout the change of light angle while white LED produces insignificant amount of output voltage. Green LED was selected as the sensing element as it has both suitable output voltage range and higher linearity on the response with the change of light angle. Under intense light source, the output voltage of green LED approaches its forward voltage drop of 1.6V when used as normal LED.

The microcontroller used has an analog to digital converter with 10-bit resolution. Both the positive and negative reference voltages of the analog to digital converter were configured to positive and negative of supply voltages which are 5V and 0V. The smallest increment that could be obtained

from the analog to digital converter with such reference voltage configuration is:

$$\frac{\text{Reference voltage}}{2^n} = \frac{5V}{2^{10}} \approx 5mV$$

Therefore, the maximum value of LED voltage that can be read by the analog to digital converter is:

$$\frac{1.6V}{0.005V} = 320$$

There are three indicator LEDs and a buzzer as the user interface added to the controller circuit as in Figure 3.11. Two of these LEDs serve as visual indication of motor turn direction. The third LED is linked with a buzzer to provide both visual and audio alert to the user, indicating battery low. This also tells the user to be ready for turn off of appliances or switch to alternative power supply for data sensitive equipment.

#### E. General microcontroller tasks

There are a total of four tasks the microcontroller has to execute repeatedly for the system to operate. These are the interrupt routine, SunTrack, ChargeManage and BatteryMonitor. When powered on or a reset has occurred, the controller program will first initialize the necessary peripherals and pins for inputs and outputs. After that the program repeatedly loops to execute SunTrack, ChargeManage and BatteryMonitor until the power has been cut off or a reset occurred. Of the three tasks in the loop, SunTrack and ChargeManage do not need to be executed frequently. Each of them has a timeout flag that signals the execution of the task after a predefined period had passed. The flags are cleared after each execution and wait for the next timeout. As reviewed in Chapter 1.1, the power drop of solar cell is almost negligible when light source is tilted below 5° from normal. This means that the adjustment of the panels could be done in intervals instead of continuous and at the same time lowers power consumption for actuating the panel. BatteryMonitor has to be executed all the time to keep the batteries in safe condition. After passing all three tasks, the program has to clear the Watchdog timer which had been setup during initialization process. The addition of Watchdog timer is to ensure that the microcontroller could reset itself should the program stops in any possible condition. As it is important for the batteries be continuously monitored for safety, the Watchdog timer provides another layer of safety by making sure the BatteryMonitor task could be executed without too much delay. **Figure 5** shows the flow chart of overall task execution process.

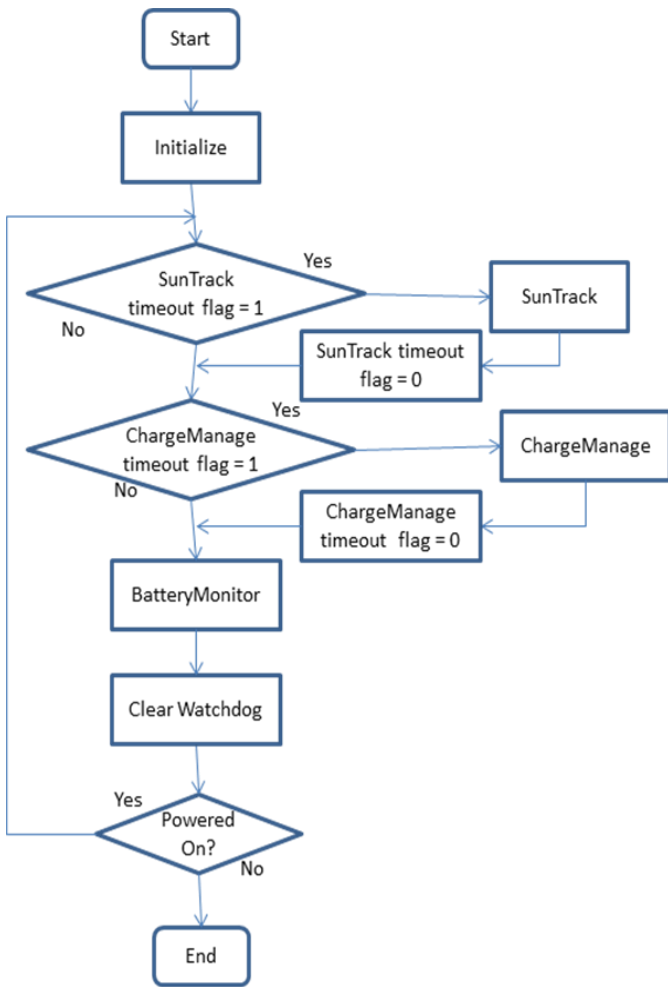


Fig. 5. Overall program flow chart

Since the acceptable tilt of light source from normal is  $5^\circ$ , the suitable interval between executions of SunTrack would be:

$$\frac{12 \text{ hours} \times 5^\circ}{180^\circ} \times 60 \text{ minutes} = 20 \text{ minutes}$$

Thus the suitable interval between executions is 20 minutes. The interval for ChargeManage was set at 30 seconds with its purpose.

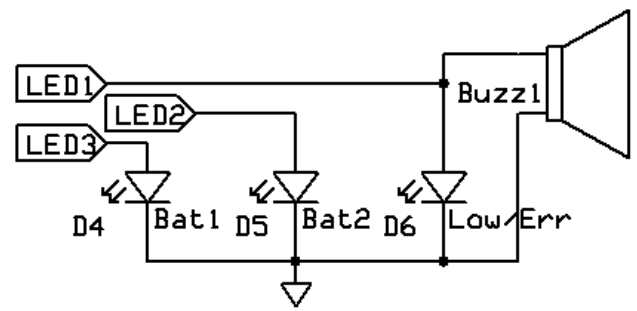


Fig. 6. Indicator LEDs and buzzer

### III. RESULT AND DISCUSSION

A small model of mirror reflection system as in Fig. 8 was built according to the sketch in Fig. 7 in order to test the feasibility of the conceptual design. The base is a piece of cardboard. Two square mirrors are the top and bottom solar panels in the simulation and are supported by four aluminum L beams by means of super glue. The side wing mirrors are held by some modeling compound to allow adjustment of angle. The internal pair of mirrors is inversely mounted to the design sketch for ease and the void between them is also filled with modeling compound. Mounting the internal pair of inverted mirrors would only invert the direction of light to the top panel bottom surface and would not affect the test result.

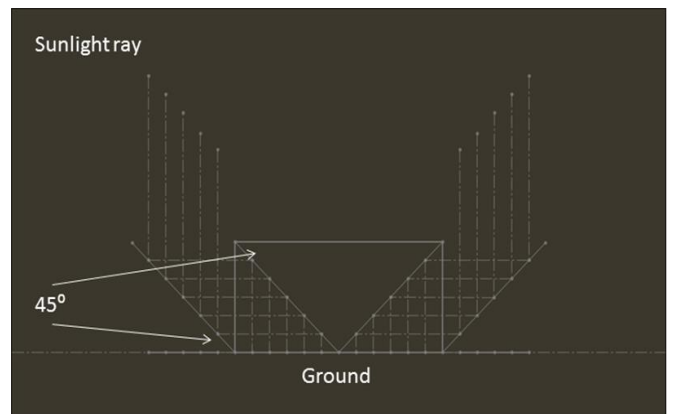
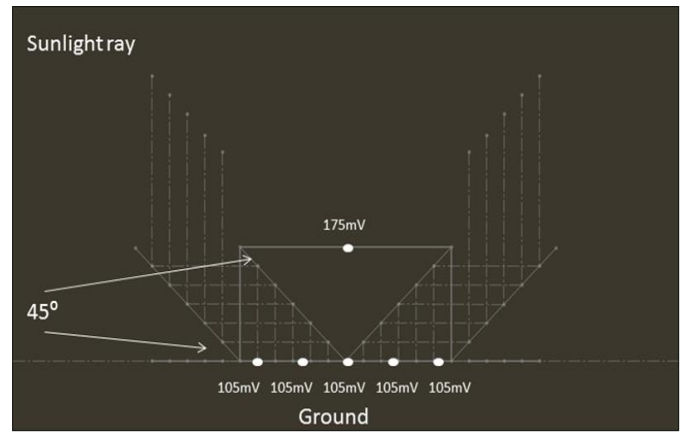


Fig. 7. Cross sectional view of the conceptual design



**Fig. 8.** Small mirror reflection system model



**Fig. 10.** Mirror reflection test result, 45° wing mirror angle, internal 45° mirror

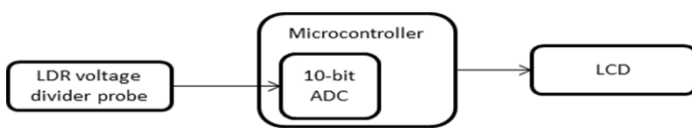


**Fig. 9.** Model measurement block diagram

The quantitative mean to compare and verify the simulated result is by measuring light brightness on multiple points on the model. The light source for the test is a constant brightness 36W fluorescent light tube placed at a fixed one meter distance over the top of the model. A light dependent resistor (LDR) configured as a voltage divider with a 1kΩ resistor was used to sense the surface light brightness by holding it as a probe on measuring surface points of the model. Measurement of the light brightness was accomplished by a microcontroller with internal 10-bit analog to digital converter (ADC) and programmed to read the received analog value from the LDR probe. Data representation was also done by interfacing an LCD to the microcontroller. The whole system will be operated with 5V power supply and the smallest increment of the 10-bit ADC at such voltage is about 5mV. The block diagram of the measurement setup is shown in **Fig. 9**.

With reference to **Fig. 10**, lights are evenly distributed across the surface of the bottom panel. In this design, the brightness loss after mirror reflection can be clearly seen. The difference of brightness between the top and bottom panels is 40%. Therefore, if the solar panels were to be designed this way, the power output difference between the two panels will also be 40%.



**Fig. 11.** Assembled new design

#### A. Sun tracking test

After the whole system was completely assembled and programmed, the unit was placed outdoor in order to test the sun tracking system. The test was conducted in a day from 9 am to 7 pm at a single location. The pictures showing the sky that the solar panels faced was captured by placing the camera on top of the panels with the lens facing up.

B. *Example power consumption scenario*

IV. CONCLUSIONS

**Table. I** : Typical power consumption of average family house lighting

House bulb location	No. of bulbs	Turn on time	Total time	Power consumed
Living room	3	7pm – 11pm	4 hours	120Wh
Dinning and kitchen	2	7pm – 8pm	1 hour	20Wh
Master bedroom	2	10pm – 12am	2 hours	40Wh
Two small bedrooms	2	10pm – 12am	2 hours	40Wh
Three bathrooms	3	Random	2 hour	60Wh

**Table I** shows the average power consumption of a four bedroom typical house. The power accumulated and stored could then be supplied to load for home usage. A usage scenario proposed was to supply the power for lighting of an average double-storey family house during the night time. In this scenario, the house was assumed to have 12 10W LED light bulbs with a schedule of their turn on time in Table I. For the house lighting described, the scenario consumed 280Wh. Total power stored in the batteries is 432Wh and considering 80% efficiency of power conversion and delivery losses with negligible usage by the system controller resulted with about 345Wh. Overall the power consumed by the house lighting is still lower than the converted and delivered power. It should be noted that the power accumulated and storage of 432Wh was recorded for a sunny day.

The concept of sun tracking and battery switching was implemented and thoroughly tested. The beneficial performance of sun tracking solar panel was observed and justified. Although, the overall project implementation was successful, the limitations and constraints slightly diminished the expected results. First of all, the pre-ordered voltage regulator IC chip was not delivered; for this reason, the prototype was constructed without the regulator. Secondly, poor weather conditions in Astana did not provide an opportunity to test the cooling capability of the proposed “V”-shaped structure and compare it with the regular shape. Lastly, the purchased batteries were of low quality; therefore, the charging process time calculation may contain discrepancies.

REFERENCES

- [1] World Energy Council. (2013) World energy resources. Available from: [http://www.worldenergy.org/wp.content/uploads/2013/09/Complete\\_WER\\_2013\\_Survey](http://www.worldenergy.org/wp.content/uploads/2013/09/Complete_WER_2013_Survey). [Accessed: 6<sup>th</sup> October 2014].
- [2] Rudisill, B. (2011) The solar resource. Available from: <http://mcensustainableenergy.pbworks.com/w/page/20638192/The%20Solar%20Resource>. [Accessed: 17<sup>th</sup> February 2016].
- [3] International Energy Agency. (2011) Solar energy perspectives. Available from: [http://www.iea.org/publications/freepublications/publication/solar\\_energy\\_perspectives\\_2011](http://www.iea.org/publications/freepublications/publication/solar_energy_perspectives_2011). [Accessed: 17<sup>th</sup> February 2016].
- [4] GAISMA. (n.d.) Astana, Kazakhstan - Sunrise, sunset, dawn and dusk times, table. Available from: <http://www.gaisma.com/en/location/astana>. [Accessed: 10<sup>th</sup> November 2014].
- [5] Ibrahim, D. (2000) Microcontroller Projects in C for the 8105. Biddles Ltd., Great Britain.
- [6] Shrivastava, S.M. (2013) Dual axis solar tracker. Gautam Budh Technical University, Lucknow, India.
- [7] SLA Battery Charging 2010, PowerStream, viewed on 17<sup>th</sup> February 2016, <http://www.powerstream.com/SLA.htm>.